How Changes in the Sequence of the Peptide CLPFFD-NH₂ Can Modify the Conjugation and Stability of Gold Nanoparticles and Their Affinity for β-Amyloid Fibrils

Ivonne Olmedo,[⊥,†] Eyleen Araya,[⊥,†,‡] Fausto Sanz,[‡] Elias Medina,[†] Jordi Arbiol,[§] Pedro Toledo,[∥] Alejandro Álvarez-Lueje,[†] Ernest Giralt,[#] and Marcelo J. Kogan*,[†]

Departamento de Química Farmacológica y Toxicológica, Facultad de Ciencias Químicas y Farmacéuticas, Universidad de Chile, Olivos 1007, Independencia, and Centro para la Investigación Interdisciplinaria Avanzada en Ciencias de Materiales, Santiago Chile, Department of Physical Chemistry, University of Barcelona, IBEC and CIBER-BB, Marti i Franques 1-13 E-08028 Barcelona, and TEM-MAT, Serveis Cientificotècnics, Universitat de Barcelona, Lluís Solé i Sabarís 1-3, E-08028 Barcelona, Spain, Chemical Engineering Department, Surface Analysis Laboratory (ASIF), University of Concepción, PO Box 160-C, Correo 3, Concepción, Chile, Institute for Research in Biomedicine, Barcelona Science Park, Baldiri Reixach 10, E-08028 Barcelona, Spain, and Departament de Química Orgànica, Universitat de Barcelona, Martí i Franquès, E-08028, Barcelona, Spain.

In a previous work, we studied the interaction of β-amyloid fibrils (Aβ) with gold nanoparticles (AuNP) conjugated with the peptide CLPFFD-NH₂. Here, we studied the effect of changing the residue sequence of the peptide CLPFFD-NH₂ on the efficiency of conjugation to AuNP, the stability of the conjugates, and the affinity of the conjugates to the Aβ fibrils. We conjugated the AuNP with CLPFFD-NH₂ isomeric peptides (CDLPFF-NH₂ and CLPDFF-NH₂) and characterized the resulting conjugates with different techniques including UV−Vis, TEM, EELS, XPS, analysis of amino acids, agarose gel electrophoresis, and CD. In addition, we determined the proportion of AuNP bonded to the Aβ fibrils by ICP-MS. AuNP-CLPFFD-NH₂ was the most stable of the conjugates and presented more affinity for Aβ fibrils with respect to the other conjugates and bare AuNP. These findings help to better understand the way peptide sequences affect conjugation and stability of AuNP and their interaction with Aβ fibrils. The peptide sequence, the steric effects, and the charge and disposition of hydrophilic and hydrophobic residues are crucial parameters when considering the design of AuNP peptide conjugates for biomedical applications.

INTRODUCTION

Present-day nanomedicine exploits carefully a broad variety of structured nanoparticles. These nanoparticles may serve as diagnostic and therapeutic antiviral, antitumor, or anticancer agents (1, 2). Metallic nanoparticles (NP) can be made so as to respond resonantly to a time-varying magnetic field, with advantageous results related to the transference of energy to the NP. For example, the particles can be made to heat up, leading to its use as a hyperthermia agent, by delivering toxic amounts of thermal energy to targeted bodies such as tumors. The NP can also act as enhanced chemotherapy and radiotherapy agents, where a moderate degree of tissue warming results in more effective destruction of malignant cells. Local heat delivered by NP selectively attached to a target can be used as *molecular surgery* to safely remove toxic and clogging aggregates. Recently, we applied this principle to protein aggregates, concretely to the protein Aβ, involved in Alzheimer's disease (3). We redissolved Aβ deposits remotely by using the local heat dissipated by gold nanoparticles (AuNP) conjugated to the peptide CLPFFD-NH₂. The resulting conjugate was selectively attached to the aggregates of Aβ, and then the system was irradiated with low gigahertz electromagnetic fields.

The determinant success in therapeutic and diagnostic use of NP is the ability to deliver them to the desired target. In this sense, NP can be coated with biological molecules to make them recognize the biological target. From the point of view of molecular recognition, peptides have a number of properties participating in ligand−receptor and protein−protein molecular interactions (4). For instance, peptides are involved in molecular recognition of antibodies, which is relevant in the field of clinical diagnosis of infectious diseases (5) and in the design of new drugs and vaccines (6).

Capping AuNP with peptides could increase stability and biocompatibility; however, recently one of the main concerns has become how peptides interact and pack on a NP surface and how the anchorage to the AuNP surface affects molecular recognition of the biological target and the stability of the AuNP (1). Thiol-based organic stabilizers have been widely used as capping agents to stabilize AuNP (7–12). In particular, Levy et al. have developed a family of peptides called CALNN that increases the stability of AuNP (13). In our case, the amphipathic peptide CLPFFD-NH₂ also has a cysteine residue (C) which contains a thiol group allowing a strong interaction with the gold surface. This interaction may be additive to that of the N-terminal primary amine, since amino groups are also known to have a strong interaction with gold surfaces (14). Moreover, it has been shown by Bellino et al. (15) that the presence of the C residue and a positively charged ammonium group in the vicinity of the thiol significantly accelerates the adsorption kinetics of thiols onto citrate-stabilized AuNP. Bare AuNPs are stabilized by citrate anions, which are common electrostatic

* Corresponding author. Marcelo J. Kogan. Phone: 5629782897, Fax: 5629782988, e-mail: mkogan@ciq.uchile.cl.
[⊥] These authors contributed equally to this work.
[†] Universidad de Chile.
[‡] Department of Physical Chemistry, University of Barcelona.
[§] Serveis Cientificotècnics, Universitat de Barcelona.
[∥] University of Concepción.
[#] Institute for Research in Biomedicine, Barcelona and Department de Química Orgànica, Universitat de Barcelona.

stabilizing agents, because the particles are typically synthesized through a citric acid reduction reaction (*13*). Electrostatic stabilization arises from mutual repulsion between neighboring AuNPs resulting from the negative surface charges of the citrate layer. Peptide CLPFFD-NH$_2$ is bound spontaneously to the AuNP replacing the citrate coating on the AuNP by forming stable Au−S bonds, as seen in the case of other peptides as CALNN (*13*).

In order to direct the AuNP to the toxic Aβ fibrils, in a previous work we conjugated AuNP to the peptide CLPFFD-NH$_2$, forming the AuNP-CLPFFD-NH$_2$ conjugate, which selectively attaches to the Aβ fibrils (*3*). This peptide is a fragment corresponding to the physiological molecule Aβ (1−42) and recognizes a particular (hydrophobic) domain of the β-sheet structure (the sequence ^{17}LVF^{20}F which is one of the hydrophobic cores of the native protein Aβ). In that work, we demonstrated that CLPFFD-NH$_2$ increases the affinity of AuNP for Aβ. The CLPFFD-NH$_2$ peptide contains at the C-terminal extreme an Asp residue (D) that confers primary amphipathicity to the molecule (i.e., in the C-terminal end of the sequence there is a polar charged residue, and following the sequence there are preponderantly hydrophobic residues), and increases the solubility of the peptide molecule. The presence of the residues Leu (L), Phe (F), and Phe (F), also present in the native sequence, confers to the molecule the ability to recognize the aggregates of Aβ (*16*).

The aim of this work is to explore the effect of changing the residue sequence of CLPFFD-NH$_2$ on the AuNP peptide conjugation, stability, and affinity to Aβ fibrils. The purpose is to modify the distances between the AuNP surface and the position of the negatively charged hydrophilic residue at pH 7.4 (i.e., the D residue).

EXPERIMENTAL PROCEDURES

Synthesis of AuNP. Citrate-coated AuNPs (12.5 ± 1.7 nm) were prepared by citrate reduction of HAuCl$_4$. An aqueous solution of HAuCl$_4$ (100 mL, 1 mM) was refluxed for 5−10 min, and a warm (50−60 °C) aqueous solution of sodium citrate (10 mL, 38.8 mM) was added quickly. Reflux was continued for another 30 min until a deep red solution appeared. The solution was filtered through 0.45 μm Millipore syringe filters to remove any precipitate, the pH was adjusted to 7.4 using dilute NaOH solution, and the filtrate was stored at 4 °C. AuNP were observed by transmission electronic microscopy (TEM) using a JEOL JEM-1010 microscope. The specimen was prepared by dropping AuNP on Formvar carbon-coated copper microgrids and letting them dry.

Peptide Synthesis. CLPFFD-NH$_2$, CDLPFF-NH$_2$, and CLP-DFF-NH$_2$ were synthesized following fluorenylmethyloxycarbonyl (Fmoc) strategy and solid-phase synthesis. Fmoc-protected amino acids were purchased from Novabiochem (Laufelfingen, Switzerland) and Perseptive Biosystems (Framingham, Massachusetts). *O*-(Benzotriazol-1-yl)-*N,N,N′,N′*-tetramethyluronium tetrafluoroborate (TBTU), Fmoc-AM handle, and resin MBHA were also obtained from Novabiochem. Chemical reagents *N,N′*-diisopropylcarbodiimide (DIPCI), 1-hydroxy-1*H*-Benzotriazole (HOBt), triethylsilane, and dimethylaminopyridine (DMAP) were from Fluka (Buchs, Switzerland). Manual synthesis including the following steps: (i) resin washing with DMF (5 × 30 s); (ii) Fmoc removal with 20% piperidine/DMF (1 × 1 min + 2 × 7 min); (iii) washing with DMF (5 × 30 s), (iv) washing with DMF (5 × 30 s) and CH$_2$Cl$_2$ (5 × 30 s); (v) Kaiser's test (with a peptide−resin sample); (vi) DMF washing (5 × 30 s). Cleavage of the peptide was carried out by acidolysis with trifluoroacetic acid (TFA) using triethylsilane and water as scavengers (94:3:3, v/v/v) for 60−90 min. TFA was removed with N$_2$ stream and the oily residue precipitated with dry *tert*-butyl ether. Peptide crude was recovered by centrifugation and decantation of the *tert*-butyl ether phase. The solid was redissolved in 10% acetic acid (AcH) and lyophilized. The peptide was analyzed by RP-HPLC [Waters 996 photodiode array detector (λ = 443 nm) equipped with a Waters 2695 separation module (Milford, MA), a Symmetry column (C18, 5 μm, 4.6 × 150 mm), and Millennium software; flow rate = 1 mL/min, gradient = 5−100% B over 15 min (A = 0.045% TFA in H$_2$O, and B = 0.036% TFA in acetonitrile)]. The peptide was purified by semipreparative RP-HPLC [Waters 2487 Dual Absorbance Detector equipped with a Waters 2700 Sample Manager, a Waters 600 Controller, a Waters Fraction Collector, a Symmetry column (C18, 5 μm, 30 × 100 mm), and Millennium software]. The peptide was finally characterized by amino acid analysis with a Beckman 6300 analyzer and by MALDI-TOF with a Bruker model Biflex III. Amino acid analysis of CLPFFD-NH$_2$: Asp 1.0 (1), Pro 0.97 (1), Leu 1.0 (1), Phe 2.03 (2) and mass spectrometry MALDI-TOF: CLPFFD-NH$_2$, [M+H$^+$]=740 and [M+Na$^+$]=762. Stock solutions of the peptides were prepared by dissolution in water. The pH was adjusted to 7.4 using concentrated NaOH, and the resulting 1.3 mM solution was filtered using 0.2 μm PVDF filters and kept as aliquots at −80 °C. An amino acid analysis (Alta Biosciences, Birmingham, U.K.) indicates a final concentration of 1.28 mM after filtering.

Conjugation of Peptides to AuNP. CLPFFD-NH$_2$, CLPDFF-NH$_2$, and CDLPFF-NH$_2$ capped AuNPs were prepared by mixing 5 nM AuNP and peptide stock solution in a volume ratio of 10 to 1. The conjugation was made in the presence of peptide excess in order to ensure full conversion of the AuNP and, consequently, homogeneous conjugation. The AuNP were afterward purified first in a 450 nm filter and then by dialysis (during three days in a membrane Spectra/Por MWCO 6−8000 against 1.2 mM sodium citrate and the solution was changed 6 times) to eliminate the excess of peptide. UV−Vis absorption spectra were recorded at room temperature with a Unicam UV/vis spectrophotometer (UV3). In order to check the absence of nonconjugated peptide, 3 mL of the conjugated solution were centrifuged at 13 500 rpm for 30 min (AuNP peptide sediments) and the supernatant was evaporated to dryness and an analysis of amino acids was carried out. On the other hand, the absence of free peptide both in the supernatant and in the NP pellet (the conjugated AuNP) was also checked by HPLC ES-MS. Separately, the NP pellet and the residue of the supernatant (after the draining) were suspended in 300 μL of 1% TFA and filtered through a 220 nm filter. In any case, the presence of the peptide was detected.

XPS. X-ray photoelectron spectroscopy (XPS) experiments were performed in a PHI 5500 Multitechnique System (from Physical Electronics) with a monochromatic X-ray source (Al Kα line of 1486.6 eV energy and 350 W), placed perpendicular to the analyzer axis and calibrated using the 3d$_{5/2}$ line of Ag with a full width at half-maximum (fwhm) of 0.8 eV. The analyzed area was a circle of 0.8 mm diameter, and the selected resolution for the spectra was 187.5 eV of pass energy and 0.8 eV/step for the general spectra and 23.5 eV of pass energy and 0.1 eV/step for the spectra of the different elements. Some measurements were done after some cleaning by sputtering the surface with an Ar$^+$ ion source (4 keV energy). All measurements were made in an ultrahigh-vacuum chamber pressure between 5 × 10^{-9} and 2 × 10^{-8} Torr.

EELS. Electron energy loss spectra (EELS) were obtained in a Gatan Image Filter (GIF 2000) coupled to the JEOL 2010F microscope, with an energy resolution of 1.2 eV.

Estimation of the Number of Peptide Molecules per AuNP. The amount of peptide molecule per NP was estimated by analysis of amino acids and absorption spectrophotometry.

The concentration of AuNP in the solutions was obtained taking into account the molar coefficient of extinction of the 12 nm diameter (5.7×10^7 M^{-1} cm^{-1}) AuNP and an analysis of amino acids of the pellet obtained after centrifugation of the conjugates at 13500 rpm for 30 min (in such conditions the NP sediment). The number of peptide molecules per AuNP was obtained by dividing the number of peptide molecules per mL of solution by the number of particles per mL of solution. This ratio was obtained in triplicate in three independent synthesis and conjugation.

Zeta Potential. The zeta potential (Zeta sizer 3000, Malvern Instruments, UK) measurements of the 12 nm diameter AuNP consisted of five repeats of each AuNP solution. The AuNP in 1.2 mM citrate solution were adjusted to pH 7.4 with a 0.1 M buffer phosphate solution, and a final buffer concentration of 10 mM. Because the zeta potential measurements were performed in an aqueous solution, the Smolouchowski approximation was used to calculate the zeta potential from measured electrophoretic mobility.

Electrophoresis. Submarine gel electrophoresis of the AuNP-peptide conjugates was performed in 1.5% agarose gels (Molecular Biology grade, Roche) using as a running 10 mM phosphate buffer in 1.2 mM sodium citrate. The field strength was held constant at 120 V and the current was 97 mA. 50 μL of AuNP solutions were mixed with 50 μL of 1:9 glycerol/buffer solution and loaded in the gels.

Stability of AuNP and Their Conjugates. (a) Characterization of NP aggregation by UV−visible Spectrometry. UV−Vis absorption spectra were recorded at room temperature with a Unicam UV/Vis spectrophotometer (UV3). The aggregation parameter (AP) was defined as follows: $AP = (A - A_0)/A_0$, where A is the integrated absorbance between 600 and 700 nm and A_0 is the integrated absorbance between 600 and 700 nm of the dispersed solution.

(b) Dialysis against water. Ten mL of the colloidal solutions of AuNP were dialyzed in 2 L of water (during 1 day in a membrane Spectra/Por MWCO 6−8000 against water, and the water was changed at 1 h and 3 h).

(c) Stability in running agarose electrophoresis with buffer solutions. 500 μL of each solution were mixed with 500 μL of phosphate buffer and the aggregation parameter (AP) was determined by UV−vis spectrophotometry.

(d) Stability in artificial cerebrospinal fluid buffer (ACSF): 124 mM NaCl, KCl 5 mM, NaH$_2$PO$_4$ 1.25 mM, MgCl$_2$ 2 mM, CaCl$_2$ 2 mM, NaHCO$_3$ 26 mM, dextrose 10 mM (see ref (17)). 50 μL of each 5 nM colloidal solution was mixed with 950 μL of ACSF buffer and the aggregation parameter (AP) was determined by UV−Vis spectrophotometry.

(e) Stability in rat serum. 50 μL of each 5 nM colloidal solution were mixed with 950 μL of serum and the aggregation parameter (AP) was determined by UV−Vis spectrophotometry. For spectrophotometric measurement, a blank with 50 μL of citrate and 950 μL of serum was used. Serum was obtained from blood collected from Sprague−Dawley male rats (200−300 g). The blood was centrifuged (at room temperature) at 3000 rpm and supernatant liquid was collected.

Circular Dichroism (CD). 150 μL of 40 nM colloidal solution was mixed with 50 μL of phosphate buffer saline and 86 μL of trifluoroethanol (TFE) were added. Circular dichroism spectra were recorded with a Jasco J700 spectropolarimeter (Great Dumnow, UK), at a spectral bandwidth of 1 nm, with a time constant of 4 s (scan speed 10 nm/min) and a step resolution of 0.2 nm. Each spectrum was the result of three accumulations and were measured at 25 °C. A blank spectrum of 150 μL of 1.2 mM citrate, 50 μL of phosphate buffer saline and 86 μL of TFE was subtracted from each conjugate spectrum. Mean residue ellipticity, $[\theta]_{MR}$, is given in units by deg·cm^2·dmol^{-1}.

Interaction with Amyloid Fibrils. (a) Preparation of Aβ_{1-42} solution. Aβ_{1-42} was purchased from Peptide Institute, Inc. (Japan). Water−peptide aliquots were lyophilized again in glass vials and stored at −20 °C until used. A variant of Zagorski's protocol was followed in order to obtain a homogeneous Aβ_{1-42} solution free from aggregates (18). Summarizing, in the same vial where it was lyophilized, Aβ_{1-42} was treated with TFA in order to eliminate any pre-existing aggregates. TFA was then evaporated under a stream of nitrogen. To thoroughly remove TFA, 1,1,1,3,3,3-hexafluoro-2-propanol was added and evaporated under a nitrogen stream. This last step was repeated three times and the sample was finally left overnight in a desiccator. The desiccated aliquot was carefully and completely resuspended in 18 μL of 10 mM NaOH per each 100 μL of final sample. Finally, 10 μL of 200 mM phosphate buffer and water was added to complete 100 μL (200 μL of the sample was prepared). All solutions are cleaned of small particles by filtration through a 0.20 μm pore size filter (Millipore). At the end of the process, Aβ_{1-42} was at a concentration of 40 μM. The solution was divided into four aliquots of 50 μL each and incubated at 37 °C for 4 h with mechanical shaking.

(b) Interaction of the samples with AuNP and the conjugates. 150 μL of 1 nM AuNP-CLPFFD-NH$_2$, AuNP-CDLPFF-NH$_2$, or AuNP-CLPDFF-NH$_2$ were added to the Aβ_{1-42} solutions and the samples were incubated for 44 additional h at 37 °C with mechanical shaking (nonmature fibrils: i.e. the 2 day old samples) or for 164 additional h at 37 °C with mechanical shaking (mature Aβ precipitated fibrils: i.e., the 7 day old samples). For TEM observations, aliquots of 1 μL of the preparations were diluted in cold (4 °C) with 20 mM PBS buffer (pH 7.4) to a final peptide concentration of 1 μM. Then, the samples were adsorbed for 1 min onto glow discharged carbon-coated colloidal films on 200 mesh copper grids. The TEM grids were then blotted and washed in Milli-Q water before negative staining with 2% uranyl acetate for visualization by TEM (JEOL JEM-1010).

(c) Quantification of gold in fibrils and supernatants. In order to separate the free and bound nanoparticles a centrifugation at 5000 rpm during 5 min was carried out. The pellet was washed with 20 mM phosphate buffer, and the first and the second supernatant were mixed. The concentration of proteins in the total supernatant was determined following the Bradford protocol. The content of gold in both pellet and supernatant was analyzed by ICP-MS after lyophilization.

(d) Determination of gold content in pellets and supernatant. The determinations were carried out in triplicate. The ICP multielement standard was obtained from high purity standards (QCS-26). Samples were digested by using a Millestone MLS-1200 Mega plus EM-45 microwave oven and following USEPA Method IO-3.1. Basically, this consists of extraction of the elements using 10 mL of a nitric acid−hydrogen peroxide (10:1) solution. After the digestion process, gold was determined directly by ICP-MS (Fisons VG-PlasmaQuad) in each fraction. The values obtained in μg/L were expressed in μg in the pellets and supernatants, and finally the ratio between gold in the supernatant (free AuNP) and in the pellet-bound AuNP were calculated. The contents of protein in the pellets of all the samples and in all the supernatants were similar, indicating that the presence of nanoparticles does not affect the fibril formation. In addition to quantify the amount of Aβ fibrils formed in the presence of the AuNPs, thioflavine T assays were performed observing that quantity of Aβ fibrils in the samples of 2 and 7 days (AuNP + fibrils, AuNP-CLPFFD-NH$_2$ + fibrils, AuNP-CDLPFF-NH$_2$ + fibrils, and AuNP-CLPDFF-NH$_2$ + fibrils)
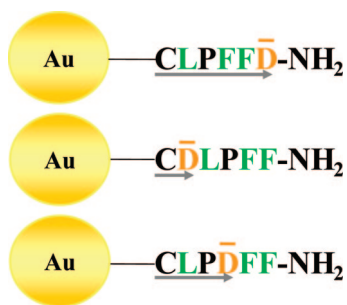
Figure 1. Schematic representation of the peptides conjugated to AuNP at physiological pH 7.4 (The calculated isoelectric point, using the software *Insight II*, of the free peptides is approximately 5.6). In orange is represented the D residues which have a formal negative charge at this pH. In green are represented the hydrophobic residues (LFF). Note that in AuNP-CLPFFD-NH$_2$ and in AuNP-CDLPFF-NH$_2$ the hydrophobic residues LFF are uninterrupted by the hydrophilic residue D, which would allow an optimal interaction with the Aβ fibrils. On the other hand, in AuNP-CLPDFF-NH$_2$ the hydrophobic residues LFF are interrupted by the hydrophilic D. The gray arrows show schematically the distance between the gold surface and the D residue assuming an extended peptide conformation.

were similar, indicating that AuNP does not interfere in the process of Aβ aggregation (data not shown).

RESULTS AND DISCUSSION

Rational Design of the Isomers of CLPFFD-NH$_2$ for Conjugation with AuNP. For pharmaceutical application of a conjugate AuNP−peptide, it is important to take into account the colloidal stability and the recognition ability of the conjugate AuNP−peptide to the desired target, in this case to the Aβ fibrils. To maintain colloidal stability, it is important that the charge of the AuNP be exposed to the bulk solution to form the double layer that stabilizes the colloid. On the other hand, for recognition purposes it is important that the hydrophobic residues on the conjugate be exposed, in this case L, F, and F residues, to the Aβ fibrils. We chose two isomers of peptide CLPFFD-NH$_2$, i.e., peptide CDLPFF-NH$_2$ and peptide CLPDFF-NH$_2$. When the peptide adopts an extended conformation, the D residue localizes away from the gold surface in the case of CLPFFD-NH$_2$, while in the case of AuNP-CDLPFF-NH$_2$, it is near the AuNP surface (Figure 1). In the case of CLPDFF-NH$_2$, an intermediate situation occurs. In conjugates AuNP–peptide, the stability of the colloid will be modulated by the exposition of the charge to form the double layer and the steric repulsion produced by the peptide capping. On the other hand, the affinity of the conjugates for Aβ fibrils will be modulated by the peptide structure and the exposition of the hydrophobic residues L, F, and F to Aβ fibrils in the cases of CLPFFD-NH$_2$ and CDLPFF-NH$_2$, in contrast to CLPDFF-NH$_2$where the L, F, and F residue sequence is interrupted by the hydrophilic charged residue D.

Synthesis and Characterization of AuNP−Peptide Conjugates. AuNP of 12.5 ± 1.7 nm in diameter (Figure 2) were synthesized by reduction of HAuCl$_4$ with sodium citrate in accord with a previous work (*13*).

The AuNP−peptide conjugates were prepared by mixing the colloidal AuNP solution with an excess of peptide to obtain a completely functionalized AuNP surface. The conjugates were exhaustively characterized by using UV−Vis spectrophotometry, EELS, XPS, amino acid analysis, gel electrophoresis, and CD. The peptides were synthesized following a solid-phase synthesis and Fmoc/tbu strategy (*19*). Several dialyses were then performed over three days in order to purge the remaining nonconjugated peptide. Figure 3 shows UV−Vis spectra of the bare AuNP and peptide conjugated to AuNP. The characteristic shift of the surface plasmon resonance band from 519 to 527 nm was observed in the conjugates.

EELS and XPS techniques were used to prove the presence of S−Au bonds on the surface. EELS spectra in the region between 50 and 240 eV were obtained on the AuNP surface from the different samples in order to evaluate the presence of sulfur, and ensure in this way the functionalization of the AuNP with the different peptides (Figure 4A). In Figure 4B, we show a detail of the electron energy loss near edge spectra (ELNES) at the S L$_{2,3}$ edge (165 eV), showing that the edge shape dramatically changes when obtaining the spectrum of the bare AuNP with regard to the peptide-functionalized AuNP. All sample spectra show the typical S L$_{2,3}$-edge slope characteristic of the peptide functionalization (Figure 4B). The spectra obtained on the surface of AuNP in samples AuNP-CLPFFD-NH$_2$ (red-line spectrum), AuNP-CDLPFF-NH$_2$ (green-line spectrum), and AuNP-CLPDFF-NH$_2$ (blue-line) present a clear edge at 165 eV, which is indicative of the presence of sulfur bonded atoms (L$_{2,3}$-edge). This last result corroborates the presence of S atoms at the Au surface, and consequently, the presence of S bonded atoms would imply the functionalization of the AuNP with the peptides in all the samples studied.

Further characterization of the colloids by XPS was performed. In Supporting Information Figure S1, we present survey spectra for four samples taken under similar conditions. In AuNP−peptide conjugates, the expected peaks from S 2p, S 2s, and Au 4f core levels were detected. High-resolution data have also been recorded in the S 2p, S 2s, and Au 4f, spectral regions (Supporting Information Figures S2, S3, and S4). The S 2p signal consists of a broad band with a maximum at 162.2 eV that corresponds to the chemisorptions of sulfur grafted onto gold (*20–23*). A similar trend is also observed with the S 2s photoelectron peak (see Supporting Information Table T1). This peak is a particularly good parameter since it is a singlet, thus making the interpretation straightforward. The S 2s photoelectron binding energy (BE) from bulk peptide with the free thiol and AuNP peptide thiolate are found at 228.2 and 227.3, respectively (Supporting Information Table 1). Similar behavior was reported by Bensebaa et al. (*24*). The accuracy of these BE values is estimated to be ±0.2 eV at the worst. In the case of bare AuNP and capped AuNP, the signal corresponding to Au 4f$_{7/2}$ is positioned at 84.2 eV (see Supporting Information Figure S4). The fact that the measured Au 4f$_{7/2}$ photoelectron BE is not detected by the sulfur chemisorption is probably because the peak separation is too small. The same result was obtained in capped AuNP with alkanethiolates (*24*).

The number of peptides per AuNP was calculated by dividing the quantity of grafted peptide (obtained by analysis of amino acids of the AuNP pellet) by the amount of AuNP in solution, which was photometrically determined (see Experimental Section). The degree of conjugation follows the order AuNP-CLPFFD-NH$_2$ > AuNP-CLPDFF-NH$_2$ > AuNP-CDLPFF-NH$_2$ (460 ± 30, 420 ± 10, and 203 ± 5 peptide molecules per AuNP). Assuming that (i) the surface of a 12.5 nm in diameter AuNP is 490 nm^2, (ii) the projection of a cylindrical peptide molecule (with cylindrical base) resting along its base on the gold surface in an extended conformation is 0.6 nm^2 (estimated by molecular modeling with the program *Insight II*), and (iii) a hexagonal close-packed lattice in which the maximum number of molecule not exceeding the packing density of 74% is 609 molecules, we conclude that our peptide molecules (for instance, only 460 in the case of AuNP-CLPFFD-NH$_2$) are not forming a compact self-assembled monolayer (SAM).

Effect of the Residue Sequence in the Stability of the AuNP−Peptide Conjugates. CLPFFD-NH$_2$, CDLPFF-NH$_2$, and CLPDFF-NH$_2$ are more stable than bare AuNP. At 4 °C, AuNP-CLPFFD-NH$_2$ and AuNP-CLPDFF-NH$_2$ do not aggregate at pH = 7.4 (in buffer phosphate 10 mM) for one year, but AuNP-CDLPFF-NH$_2$ and bare AuNP do (see Supporting
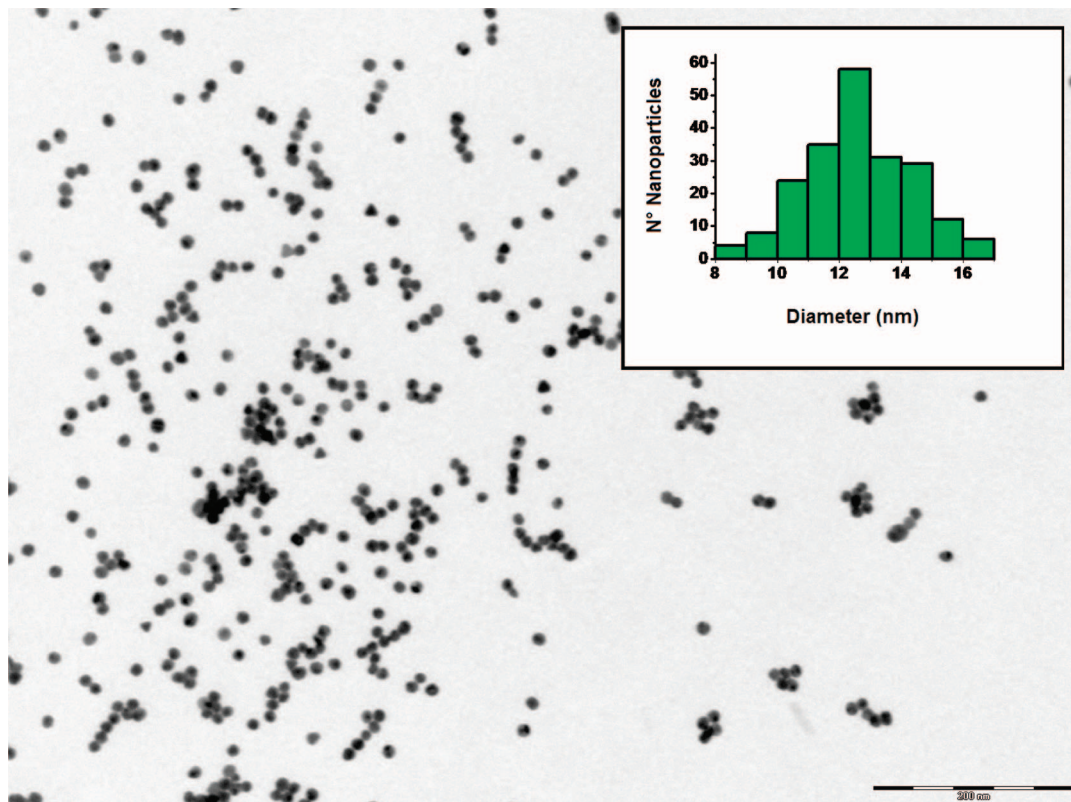
Figure 2. TEM micrograph of AuNP. The insert shows the distribution diameter of the AuNP.
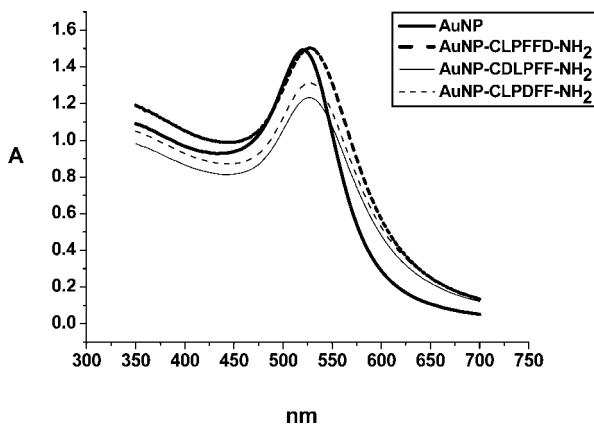
**Figure 3.** UV−vis spectra of bare AuNP and peptide-capped AuNP.

Information Figure S5). Peptide stabilization of AuNP is a documented phenomenon (*1*), although the effect of the peptide sequence in the stability has been documented for only the peptide CALNN (*13*).

In order to evaluate the stability of the AuNP−peptide conjugates, we measured the UV−Vis spectra for different conditions and determined the AP, in the way defined by Levy et al. (ref (*13*); see Experimental Section). The stability of the AuNP and their conjugates was studied both after fast freezing/defreezing (Figure 5A) and after fast freezing/freeze-drying and reconstitution in water (Figure 5B). AuNP-CLPFFD-NH$_2$ and AuNP-CLPDFF-NH$_2$ were more stable than AuNP-CDLPFF-NH$_2$ and bare AuNP in both conditions (Figure 5A,B). These results also reveal higher exposition of the hydrophobic residues F and F to the solvent (10 mM phosphate buffer, pH 7.4 in 1.2 mM sodium citrate) in the case of AuNP-CDLPFF-NH$_2$ than in the cases AuNP-CLPFFD-NH$_2$ and AuNP-CLPDFF-NH$_2$, a direct consequence of having the F groups in the conjugate AuNP-CDLPFF-NH$_2$ located far from the influence of the

charged aspartic group. Thus, after freezing, the hydrophobic groups of AuNP-CDLPFF-NH$_2$ particles freely interact through van der Waals interactions (excluding water) producing aggregation and subsequent colloid flocculation.

In colloids there are several interactions that determine the stability. The combination of van der Waals attractive forces and steric forces form the basis for the theory of steric stabilization. Fine particles tend to attract each other due to van der Waals attractive forces that can be neutralized through the addition of charge and/or grafting molecules onto the nanoparticle surface. In the first case, stabilization occurs due to electrostatic repulsion, while in the second case, stabilization occurs due to steric repulsive forces (*25*). Here, we report on two parameters related to the nanoparticle charge, the zeta potential and migration in an electrophoresis gel.

Effect of the Residue Sequence on the Charge of the AuNP−peptide Conjugate. The classical Derjaguin-Landau-Verwey-Overbeekn (DLVO) theory has been widely employed in colloid science for understanding colloidal interaction in liquids (*26–28*). The salient feature of the theory indicates that a colloidal system remains stable if repulsion forces dominate particle interactions over attractive van der Waals forces. However, when attractive forces dominate, then colloidal particles cluster together forming flocculates and aggregates. The origin of stabilizing repulsion forces may be Coulombic, entropic arising from the confinement of thermally mobile surface groups, or a combination. Higher (absolute) values of zeta potentials yield stronger Coulombic repulsion between the particles, thus diminishing the impact of the van der Waals force attractions. Table 1 summarizes the zeta potentials corresponding to bare AuNP and AuNP−peptide conjugates. In general, AuNP−peptide conjugates present lower zeta potential (absolute) values than bare AuNP. We attribute this to the replacement of ion citrates (ion citrates have three dissociated negatively charged carboxylic groups at pH 7.4) with peptide molecules (which bear one formal negative charge at pH 7.4). For instance,
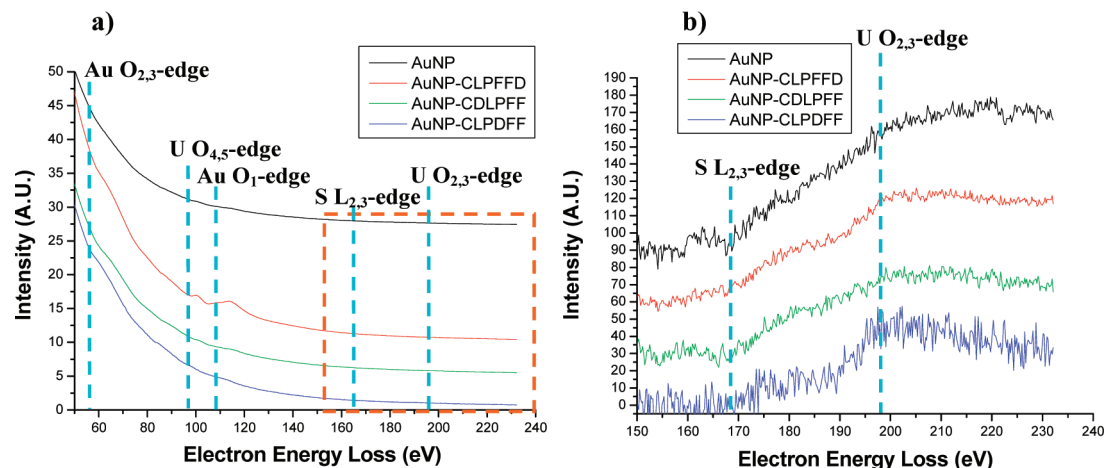
Figure 4. (A) EELS spectra obtained on the surface of 12.5 nm sized AuNP, nonfunctionalized (black line), and functionalized with different peptides (red, blue, and green spectra). (B) Detail of the S $L_{2,3}$ ELNES spectra obtained from the spectra showed in a. Au $O_{2,3}$-edge 54 eV; Au O_1-edge 83 eV; U $O_{4,5}$-edge 96 eV; U $O_{2,3}$-edge 195 eV; S $L_{2,3}$-edge 165 eV.

Table 1. Zeta Potential of Bare and AuNP–peptide Conjugates at pH 7.4 (10 mM phosphate buffer pH 7.4, in 1.2 mM citrate)[a]

colloid	zeta potential mV (std. dev. in mV)
AuNP	−54.3 (2.9)
AuNP-CLPFFD-NH$_2$	−43.7 (1.5)
AuNP-CDLPFF-NH$_2$	−34.9 (0.6)
AuNP-CLPDFF-NH$_2$	−42.8 (1.0)

[a] Low std dev in all cases suggests homogeneous zeta potential distribution and thus capping degree.

the replacement of one peptide molecule with one citrate ion will reduce the total negative charge of the AuNP in two units. However, the diminution of the charge density is not always accompanied by an increase in the peptide grafting density. Remarkably, in the case of AuNP-CDLPFF-NH$_2$ in which the quantity of peptide molecules covering the surface is lower with respect to the other isomers (203 versus approximately 400 in the other two cases), the zeta potential is lower than that for the other conjugates. In this case, the presence of a carboxylate group belonging to the D residue situated near the surface, seems to induce the exclusion of more molecules of adsorbed citrate (due to the repulsive interaction between D residues and citrate carboxylates) with respect to the other conjugates.

Zeta potential values explain the higher stability of AuNP-CLPFFD-NH$_2$ and AuNP-CLPDFF-NH$_2$ with respect to AuNP-CDLPFF-NH$_2$. Even though in general AuNP–peptides present lower zeta potential values (absolute) with respect to bare AuNPs, the first are more stable than the latter possibly due to the steric stabilization produced by the peptide molecules.

Colloid stability of AuNP–peptide conjugates is enhanced by entropic repulsive interactions of the protruding peptide groups on the particles in water; these groups should not be considered as fixed or rigid, but rather as a superficial layer of flexible segments that expand or collapse on the surface. In this way, van der Waals attractive forces can be neutralized thorough the chemisorption of peptide molecules on the colloid surface and stabilization occurs due to steric repulsive forces as was described for other molecules adsorbed on nanoparticle (25, 29). So, the experimental stability order AuNP-CLPFFD-NH$_2$ > AuNP-CLPDFF-NH$_2$ > AuNP-CDLPFF-NH$_2$ > AuNP would correspond with peptide functionalization that is AuNP-CLPFFD-NH$_2$ > AuNP-CLPDFF-NH$_2$ > AuNP-CDLPFF-NH$_2$ and bare AuNP.

We also ran an electrophoresis agarose gel in phosphate buffer at pH 7.4 (10 mM) (the same conditions under which we studied the interaction with Aβ fibrils; see below). In such conditions the electrophoretic relative mobilities of the nanoparticles follow

the order AuNP-CLPFFD-NH$_2$ $\cong$ AuNP-CLPDFF-NH$_2$ > AuNP-CDLPFF-NH$_2$ > bare AuNP (Figure 6). It is important to mention that bare AuNP presented aggregation in the running conditions in contrast with the AuNP–peptide conjugates. Other works in the literature show that bare AuNP does migrate in agarose gel; however, it does when stabilized with phosphines, compounds which are different from the citrate used here (30). On the other hand, the lower mobility of AuNP-CDLPFF-NH$_2$ with respect to the other conjugates we attribute to the lower resulting surface charge produced by the exclusion of citrate molecules from the surfaces (see previous section). In the case of bare AuNP, particles aggregate (in Figure 6 see the dark coloration corresponding to AuNP in the sample loading position) no matter their high zeta potential (Table 1). This reason is unclear to us; undesired interaction of the citrate ions with the buffer (during the running) in not discarded at this point.

From a pharmaceutical point of view, it is important to determine the stability of AuNP in the absence of citrate, simply because this salt is not present in biological medium. Here, we study the stability of the conjugates and bare AuNP after deprivation of the citrate ion in the media.

Stability of AuNP and Their Conjugates after Citrate Ion Deprivation. The citrate ions play an important role in the stability of the AuNP colloids; however, the interaction of these ions with the gold surface is weak. In the conjugation process of the peptides containing thiols, there is a replacement of citrate ions by peptide molecules forming a stable binding. However, the replacement is not complete because the AuNPs are not capped with a compact SAM; thus on the surface of the AuNP, there are citrate ions and peptide molecules that together contribute to form the stabilizing double layer. To evaluate the stability of AuNP and AuNP–peptide conjugates after citrate ion deprivation, we performed a dialysis against water for 24 h. This deprivation is caused by desorption due to the diffusion process of citrate ions outside the membrane dialysis to equilibrate the chemical potential of AuNP that to the solution. We choose this way to eliminate the citrate in order to avoid centrifugation and reconstitution in a buffer media because a certain degree of aggregation could occur after centrifugation.

After deprivation of the citrate ions, the system reaches thermodynamic equilibrium concentrations inside and outside the membrane; the AP for the AuNP and AuNP–peptide was determined by spectrophotometry after 24 h of dialysis against water. AuNP were unstable (AP = 3.40 ± 0.97) which could be attributed to desorption of weakly interacting adsorbed citrate
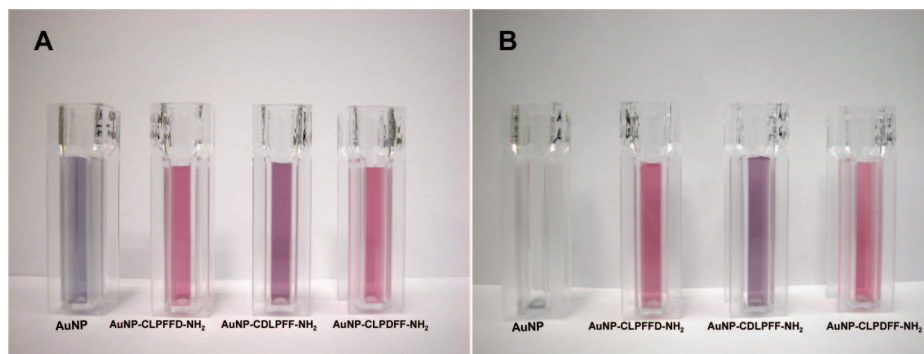
Figure 5. Photographies of colloidal solutions of bare AuNP and conjugated AuNP after: (A) freezing and defreezing and reconstitution in water (AP: 0.09 ± 0.03 for AuNP-CLPFFD-NH$_2$ and 0.06 ± 0.01 of AuNP-CLPDFF-NH$_2$, 0.45 ± 0.06 for AuNP-CDLPFF-NH$_2$, and 5.37 ± 0.24 for bare AuNP). (B) After freezing and freeze-drying the colloidal solutions and reconstitution in water (AP: 0.10 ± 0.05 for AuNP-CLPFFD-NH$_2$ and 0.14 ± 0.16 for AuNP-CLPDFF-NH$_2$, 0.35 ± 0.13, for AuNP-CDLPFF-NH$_2$ and for bare AuNP the AP could not be determined because the sample was totally precipitated).
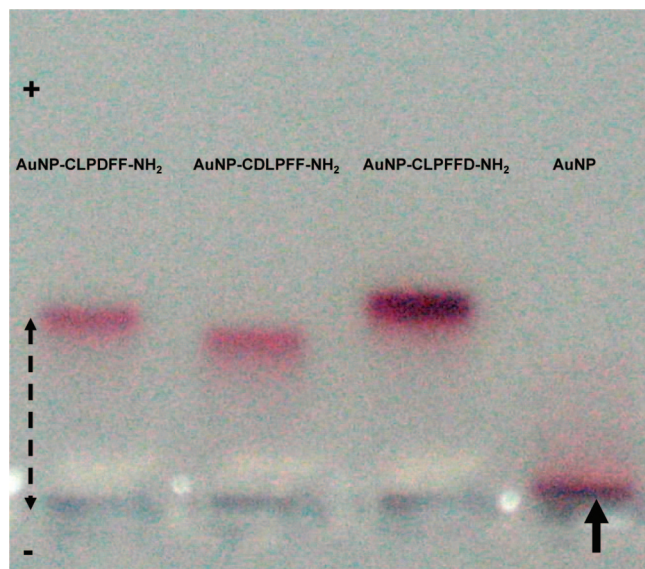
Figure 6. Electrophoresis of AuNP and AuNP−peptide conjugates in agarose gel. Run was performed in 10 mM phosphate buffer pH 7.4 in 1.2 mM citrate at 120 V for 8 min. The arrow indicates the loading sample position of AuNP. The dotted arrow indicates a real distance of 1.5 cm.

ions, which in turn leads to flocculation. AuNP-CDLPFF-NH$_2$ was also unstable, turning the determination of AP impossible. In contrast, AuNP-CLPFFD-NH$_2$ and AuNP-CLPDFF-NH$_2$ (AP $= 0.15 \pm 0.01$ and 0.73 ± 0.01, respectively) were more stable than AuNP and AuNP-CDLPFF-NH$_2$. The higher stability of AuNP-CLPFFD-NH$_2$ and AuNP-CLPDFF-NH$_2$ with respect to AuNP-CDLPFF-NH$_2$ could be attributed to the higher degree of stable functionalization confered to the AuNP surface, which protects the conjugate against citrate deprivation. Exposition of carboxylic groups belonging to the D residues increases repulsion between the nanoparticles ensuring colloidal stability. In contrast, in AuNP-CDLPFF-NH$_2$, the degree of functionalization is low, thus leading to low protection against citrate deprivation; as a result, aggregation inevitably occurs due mainly to interaction of hydrophobic groups to exclude water.

The stability of nanoparticles in biological fluids is an important issue for its practical application. We studied the stability of the nanoparticles in less artificial conditions, as in the case of ACSF, a typical buffer used for neurophysiological studies (*17*), and in rat serum.

Stability of AuNP and Their Conjugates in a Medium that Mimics Cerebrospinal Fluid. We determined the AP of bare and capped AuNPs incubated for 48 h, at 4 °C. 5 nM

AuNPs were diluted in AuNP/ACSF buffer (1:20). Figure 7 shows that only AuNP-CLPFFD-NH$_2$ were stable (AP $= 0.05 \pm 0.01$) in ACSF, while the other conjugates and bare AuNP were unstable in such conditions (AP could not be determined due to precipitation).

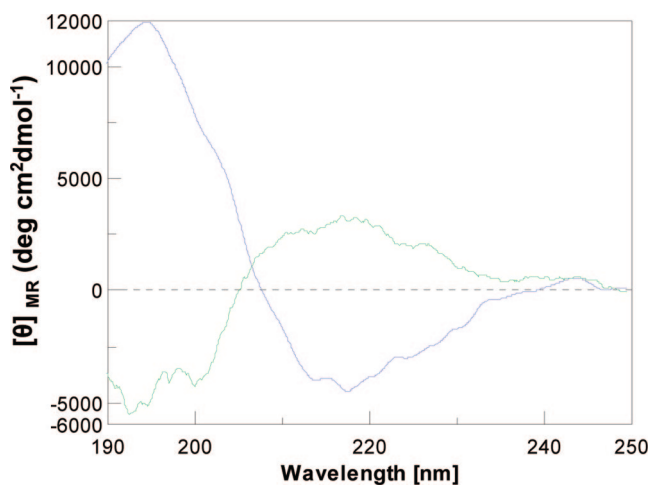**Stability of AuNP and Their Conjugates in Rat Serum.** The AP of bare and capped AuNP was determined in rat serum. The nanoparticle samples were diluted in serum in a 1:20 ratio (nanoparticle/serum) and UV−Vis spectra were obtained (Supporting Information S6). After 48 h, all the samples were stable. It should be noted that a bathochromic shift in all cases was observed before starting incubation ($t = 0$ h). This shift and stability of all samples could be attributed to nanoparticle capping with serum proteins that stabilizes the colloidal particles.

The secondary structure that adopts the peptide molecules onto the AuNP surface is related to both process, the grafting and the interaction of the anchored peptide molecules with amyloid aggregates. We carried out CD spectra of the conjugates in order to obtain information about the influence of the sequence on the structure of the peptides conjugated to AuNP.
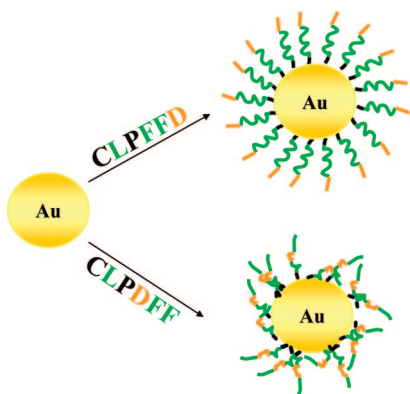
CD Spectra of Conjugates AuNP−Peptide. In an attempt to characterize the possible differences in the secondary structures of the different peptides attached to the surface of AuNP, we have recorded the CD spectra of the conjugates. In the case of CDLPFF, this measurement was not possible due to the weak contribution of peptide yielded by the low degree of AuNP functionalization. On the contrary, Figure 8 shows the CD spectra of AuNP-CLPFFD-NH$_2$ and AuNP-CLPDFF-NH$_2$. In the first conjugate, a β structure is present, while a disordered structure is found in the second conjugate. In accordance with our CD experiments, a *hypothetical* model is proposed (Figure 9) that allows visualization of how CLPFFD-NH$_2$ is grafted on the AuNP surface, allowing the accommodation of a higher number of peptide molecules in relation to the isomer CLPDFF-NH$_2$. In the case of the peptide CLPFFD-NH$_2$, which presents primary amphipathicity (*31*), the hydrophilic head (D) is far from the surface and the peptide tends to adopt an extended β conformation. The molecules are orthogonally oriented to the AuNP surface, exposing the D and avoiding the interaction between the gold surface and the terminal amide. This behavior was recently proposed by Pomerantz et al. for the deposit of amphiphilic β-peptides onto gold surfaces (*32*). In the case of peptide CLPDFF-NH$_2$, in which the primary amphipathicity is not well-defined because the D group is intercalated in the sequence between the hydrophobic residues, the peptide molecules adopt a disordered structure and fewer molecules could be accommodated onto the gold surface. In this case, the terminal amide group could be in contact with the gold surface as proposed for non-amphipathic structures (*32*).

Figure 7. Photographs of colloidal solutions of bare AuNP and conjugated AuNP after incubation in ACSF for 48 h at 4 °C (AP, 0.05 ± 0.01 for AuNP-CLPFFD-NH₂; for bare AuNP and other conjugates, the AP could not be determined because the sample was totally precipitated).
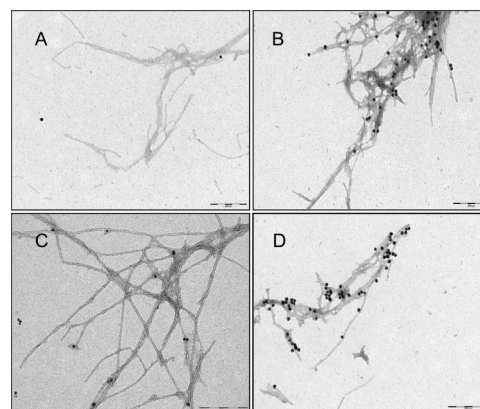

Figure 8. Far-UV CD spectra of AuNP-CLPFFD-NH$_2$ (blue) and AuNP-CLPDFF-NH$_2$(green) at pH = 7.4.

Figure 10. TEM micrograph of 7 day old amyloid fibrils stained with uranil acetate incubated with (A) AuNP, (B) AuNP-CLPFFD-NH$_2$, (C) AuNP-CDLPFF-NH$_2$, and (D) AuNP-CLPDFF-NH$_2$. Bars represent 200 nm.

to form mature fibrils. In both cases of samples, bare AuNP showed by TEM low degree of interaction with the fibril while the three AuNP−peptide conjugates showed a higher degree of interaction (Figure 10). This result could be explained by the presence of hydrophobic groups L, F, and F present in the peptides that which are able to recognize the hydrophobic nucleus in Aβ.

To quantitatively evaluate the affinity or adhesion of each conjugate to the Aβ fibril, we centrifuged the corresponding sample at 2300 *g* for 5 min; under such conditions, the unbound free AuNP remained suspended but the Aβ fibrils bound to AuNP did precipitate forming a pellet. The gold content both in the pellets and in the supernatants was determined by ICP-MS. Gold content ratios between that in the supernatant (unbound free AuNP) and that in the pellet (AuNP attached to the fibrils) are summarized in Table 2. The conjugate AuNP-CLPFFD-NH$_2$ adheres better to Aβ fibrils than the other conjugates. According to CD results, this peptide adopts a β secondary structure, which could favor the interaction of the residues L F F with Aβ fibrils. In addition, the presence of D groups at the C-terminal position produces the repulsion needed to maintain the peptide chain separation, avoiding self-aggregation between the peptide molecules conjugated to the AuNP. Thus, the adhesive interaction between the conjugate and the Aβ fibril becomes possible. Moreover, the stability of this conjugate in ACSF

Figure 9. Hypothetical cartoon based on CD results. The hydrophobic groups are represented in green and the hydrophilic groups in orange. In the case of AuNP-CLPFFD-NH₂, the peptide is oriented orthogonally to the gold surface adopting a β secondary structure, while in AuNP-CLPDFF-NH₂, the peptide is in a disordered structure. Note that in the first the degree of functionalization and exposition of D is higher than in the case of AuNP-CLPDFF-NH₂. The scale of the molecules is not in proportion with the nanoparticles.

Interaction of AuNP and AuNP−Peptide Conjugates with Aβ Fibrils. To determine the affinity of AuNP−peptide conjugates for Aβ fibrils, we incubated Aβ with AuNP and their conjugates, for 2 days to form immature fibrils and for 7 days

Table 2. Proportion of Unbound Gold (AuNP in the supernatant) and Gold Bound to the Aβ fibrils (AuNP in the pellet)[a]

	ratio of gold (supernatant/pellet) (2 d)	ratio of gold (supernatant/pellet) (7 d)
AuNP + Fibrils	6.50 ± 0.05	0.21 ± 0.05
AuNP-CLPFFD +Fibrils	1.50 ± 0.01	0.03 ± 0.02
AuNP-CDLPFF + Fibrils	3.51 ± 0.03	0.11 ± 0.02
AuNP-CLPDFF + Fibrils	3.03 ± 0.03	0.12 ± 0.05

[a] The pellet was washed with 10 mM phosphate buffer pH 7.4 in 1.2 mM citrate and centrifuged (both supernatants were mixed). The pellets and the suppernatants were lyophilized. The gold content in the pellets and in the supernatants was determined by ICP-MS.

and serum is a very important factor in future biomedical applications.

Several conclusions can be drawn from this set of experiments. The peptide sequence influences the degree of conjugation, the stability, and the interaction of AuNP−peptide conjugates. In our opinion, there are two critical factors to be considered: the position of the negative charge and the capacity to adopt a secondary structure. The position of the negative charge could be related with the colloidal stability. In the case of AuNP-CLPFFD-NH$_2$, the D residues could be located in a more external position contributing to repulsion between particles increasing the colloidal stability. On the other hand, CLPFFD-NH$_2$ anchored to the AuNP adopts a β secondary structure increasing the ability to interact with Aβ. Following the hypothetical model proposed in Figure 9, the higher number of peptide molecules are accommodated on the surface producing steric hindrance which contribute to colloidal stability. In contrast in the isomer CLPDFF-NH$_2$, the peptide adopts a more disordered structure avoiding the accommodation of molecules, reducing the degree of functionalization, the stability, and the affinity for Aβ.

The results obtained here provide a first answer to the important concern of the way bioactive peptides could allocate once they are anchored to AuNP surface and the way conjugates could interact with the biological target. However, to determine the conformation of a peptide molecule on the AuNP surface, further experiments are now in progress in our laboratory. Due to the importance that AuNP have in therapy and diagnosis, it is very helpful to understand the parameters governing the stability and interaction with the therapeutic target.

Supporting Information Available: Additional data as described in the text. This material is available free of charge via the Internet at http://pubs.acs.org.

LITERATURE CITED

(1) Kogan, M. J., Olmedo, I., Hosta, L., Guerrero, A. R., Cruz, L. J., and Albericio, F. (2007) Peptides and metallic nanoparticles for biomedical applications. *Nanomedicine 2*, 287–306.

(2) De la Fuente, J., and Berry, C. C. (2005) Tat peptide as an efficient molecule to translocate gold nanoparticles into the cell nucleus. *Bioconjugate Chem. 16*, 1176–1180.

(3) Kogan, M. J., Bastus, N. G., Amigo, R., Grillo-Bosch, D., and Araya, E. (2006) Nanoparticle-mediated local and remote manipulation of protein aggregation. *Nano Lett. 6*, 110–115.

(4) Efremov, R. G., Chugunov, A. O., Pyrkov, T. V., Priestle, J. P., Arseniev, A. S., and Jacoby, E. (2007) Molecular lipophilicity in protein modeling and drug design. *Curr. Med. Chem. 14*, 393–415.

(5) Naz, R. K., and Dabir, P. (2007) Peptide vaccines against cancer, infectious diseases, and conception. *Front. Biosci 12*, 1833–1844.

(6) Cruz, L. J., Iglesias, E., Aguilar, J. C., Cabrales, A., Reyes, O., and Andreu, D. (2004) Different immune response of mice immunized with conjugates containing multiple copies of either consensus or mixotope versions of the V3 loop peptide from human immunodeficiency virus type. *Bioconjugate Chem. 15*, 1110–1117.

(7) Hostetler, M. J., and Murray, R. W. (1997) Colloids and self-assembled monolayers. *Curr. Opin. Colloid Interface Sci. 2*, 42–50.

(8) Templeton, A. C., Wuelfing, M. P., and Murray, R. W. (2000) Monolayer-protected cluster molecules. *Acc. Chem. Res. 33*, 27–36.

(9) Whetten, R. L., Shafigullin, M. N., Khoury, J. T., Schaaff, T. G., Vezmar, I., Alvarez, M. M., and Wilkinson, A. (1999) Crystal structures of molecular gold nanocrystal arrays. *Acc. Chem. Res. 32*, 397–406.

(10) Brust, M., and Kiely, C. J. (2002) Some recent advances in nanostructure preparation from gold and silver particles: A short topical review. *Colloids Surf., A 202*, 175–186.

(11) Brust, M., and Kiely, C. J. (2004) Monolayer Protected Clusters of Gold and Silver. *Colloids and colloid assemblies* (Caruso, F., Ed.) pp 96−119, Wiley-VCH, Weinheim.

(12) Daniel, M. C., and Astruc, D. (2004) Gold nanoparticles: assembly, supramolecular chemistry, quantum-size related properties, and applications towards biology, catalysis and nanotechnology. *Chem. Rev. 104*, 293–346.

(13) Levy, R., Thanh, N. T. K., Doty, R. C., Nichols, R. J., Schiffrin, D. J., Brust, M., and Fernig, D. G. (2004) Rational and combinatorial design of peptide as capping ligands for gold nanoparticles. *J. Am. Chem. Soc. 126*, 10076–10084.

(14) Zhang, J., Chi, Q., Nielsen, J. U., Friis, E. P., Andersen, J. E. T., and Ulstrup, J. (2000) Two-dimensional cysteine and cystine cluster networks on Au(111) disclosed by voltammetry and in situ scanning tunneling microscopy. *Langmuir 16*, 7229–7237.

(15) Bellino, M. G., Calvo, E. J., and Gordillo, G. (2004) Adsorption kinetics of charged thiols on gold nanoparticles. *Phys. Chem. Chem. Phys. 6*, 424–428.

(16) Soto, C., Kindy, M. S., Baumann, M., and Frangione, B. (1996) Inhibition of Alzheimer's amyloidosis by peptides that prevent beta-sheet conformation. *Biochem. Biophys. Res. Commun. 226*, 672–680.

(17) Rozas, C., Frank, H., Heynen, A. J., Morales, B., Bear, M. F., and Kirkwood, A. (2001) Developmental inhibitory gate controls the relay of activity to the superficial layers of the visual cortex. *J. Neurosci. 21*, 6791–6801.

(18) Zagorski, M. G., Yang, J., Shao, H. Y., Ma, K., Zeng, H., and Hong, A. (1999) Methodological and chemical factors affecting Aβ amyloidogenicity. *Method Enzymol. 309*, 189–204.

(19) Dörner, B., Ostresh, J. M., Houghten, R. A., Frank, R., Tiepold, A., Fox, J. E., Bray, A. M., Ede, N. J., James, I. W., Wickham, G. (2000) Manual multiple synthesis methods, 1. Simultaneous multiple peptide synthesis - the T-bag method. *Fmoc Solid Phase Peptide Synthesis - A Practical Approach* (Chan, W. C., and White, P. D., Eds.) pp 303−327, Oxford University Press, Oxford.

(20) Brust, M., Walker, M., Bethell, D., Schiffrin, D. J., and Whyman, R. J. (1994) Synthesis of thiol-derivatized gold nanoparticles in a 2-phase liquid system. *Chem. Soc.: Chem. Commun. 7*, 801–802.

(21) Leff, D. V., Ohara, P. C., Heath, J. R., and Gelbart, W. M. (1995) Thermodynamic control of gold nanocrystal size: experiment and theory. *J. Phys. Chem. 99*, 7036–7041.

(22) Badia, A., Singh, S., Demers, L., Cuccia, L., Brown, G. R., and Lennox, R. B. (1996) Self-assembled monolayers on gold nanoparticles. *Chem. Eur. J. 2*, 359–363.

(23) Bishop, A. R., and Nuzzo, R. G. (1996) Self-assembled monolayers: Recent developments and applications. *Curr. Opin. Colloid Interface Sci. 1*, 127–136.

(24) Bensebaa, F., Zhou, Y., Deslandes, Y., Kruus, E, and Ellis, T. H. (1998) XPS study of metal-sulfur bonds in metal-alkanethiolate materials. *Surf. Sci. 405*, L472–L476.

(25) Zaman, A. A. (2000) Effect of polyethylene oxide on the viscosity of dispersion of charged silica particles: interplay between rheology, adsorption, and surface charge. *Colloid Polym. Sci. 278*, 1187–1197.

(26) Hunter, R. J. (1995) *Foundations of Colloid Science.* Oxford Sci. Pub, Clarendon Press, Oxford, U.K.

(27) Verwey, E. J. W., Overbeek, J. Th. G. (1999) *Theory of the Stability of Lyophobic Colloids*, Dover, Mineola, NY.

(28) Lee, K., Sathyagal, A. N., and McCormick, A. V. (1998) A closer look at an aggregation model of the Stöber process. *Colloids Surf., A 144*, 115–125.

(29) Ishikawa, Y., and Katoh, Y., OhshimaH. (2005) Colloidal stability of aqueous polymeric dispersions: Effect of pH and salt concentration. *Colloids Surf., B 42*, 53–58.

(30) Sandstrom, P., and Akerman, B. (2004) Electrophoretic properties of DNA-modified colloidal gold nanoparticles. *Langmuir 20*, 4182–4186.

(31) Fernandez-Carneado, J., Kogan, M. J., Pujals, S., and Giralt, E. (2004) Amphipathic peptides and drug delivery. *Biopolymers 76*, 196–203.

(32) Pomerantz, W. C., Cadwell, K. D., Hsu, Y-J., Gellman, S. H., and Abbott, N. L. (2007) Sequence dependent behavior of amphiphilic β-peptides on gold surfaces. *Chem. Mater. 19*, 4436–4441.